

Determination of the turbulent parameter in accretion disks: effects of self-irradiation in 4U 1543–47 during the 2002 outburst

G. V. Lipunova^{1*}, K. L. Malanchev^{1,2}

¹ *Moscow Lomonosov State University, Sternberg Astronomical Inst., Universitetski pr. 13, Moscow 119234, Russia*

² *Moscow Lomonosov State University, Faculty of Physics, Leninskie Gory, 1, Moscow 119234, Russia*

2 October 2023

ABSTRACT

We investigate the viscous evolution of the accretion disk in 4U 1543–47, a black hole binary system, during the first 30 days after the peak of the 2002 burst by comparing the observed and theoretical accretion rate evolution $\dot{M}(t)$. The observed $\dot{M}(t)$ is obtained from spectral modelling of the archival RXTE/PCA data. Different scenarios of disk decay evolution are possible depending on a degree of self-irradiation of the disk by the emission from its centre. If the self-irradiation, which is parametrized by factor C_{irr} , had been as high as $\sim 5 \times 10^{-3}$, then the disk would have been completely ionized up to the tidal radius and the short time of the decay would have required the turbulent parameter $\alpha \sim 3$. We find that the shape of the $\dot{M}(t)$ curve is much better explained in a model with a shrinking high-viscosity zone. If $C_{\text{irr}} \approx (2-3) \times 10^{-4}$, the resulting α lie in the interval 0.5–1.5 for the black hole masses in the range 6–10 M_{\odot} , while the radius of the ionized disk is variable and controlled by irradiation. For very weak irradiation, $C_{\text{irr}} < 1.5 \times 10^{-4}$, the burst decline develops as in normal outbursts of dwarf novae with $\alpha \sim 0.08-0.32$. The optical data indicate that C_{irr} in 4U 1543–47 (2002) was not greater than approximately $(3-6) \times 10^{-4}$. Generally, modelling of an X-ray nova burst allows one to estimate α that depends on the black hole parameters. We present the public 1-D code FREDDI to model the viscous evolution of an accretion disk. Analytic approximations are derived to estimate α in X-ray novae using $\dot{M}(t)$.

Key words: accretion – accretion disks – binaries: general – methods: numerical – X-rays: individual: 4U 1543–47

1 INTRODUCTION

The viscosity in the accretion disks is explained by the magneto-hydrodynamic (MHD) turbulence, developing due to the magneto-rotational instability (Hawley & Balbus 1991; Velikhov 1959; Chandrasekhar 1961). MHD simulations of the turbulence have been generally providing the turbulent parameter $\alpha \sim 0.01$. More recently, numerical simulations have achieved a value of $\alpha \sim 0.1$ for the regions with the partial ionization and convection (Hirose et al. 2014). Yet observations sometime indicate higher values: $\alpha \sim 0.1-0.4$ (King et al. 2007), 0.5–0.6 (Suleimanov et al. 2008; Malanchev & Shakura 2015). In this work, we study in detail an outburst of one X-ray nova and derive constraints on α .

The thermal instability in the zone of partial ionization of hydrogen in an accretion disk around a compact star is believed to be a trigger mechanism of outbursts in X-ray novae. The Disk Instability Model (DIM) was originally put forward to explain dwarf nova outbursts (see reviews by Smak 1984b; Lasota 2001). The accumulation of mass in the cold disk (where the effective temperature is

$\lesssim 10^4$ K and the matter is not ionized) between bursts leads to the situation when the surface density exceeds a critical value, and the transition to the hot state occurs on the thermal timescale. As the model predicts, this happens first at some radius, proceeding then to other disk rings outwards and inwards as an ‘avalanche’ and converting the disk to the hot state. The viscous evolution of the disk leads to an increase of the central accretion rate, which is observed as an X-ray outburst if the central body is a compact object. To reproduce outburst cycles of dwarf and X-ray novae, the α -parameter should be higher in the hot state by 1–2 orders of magnitude than in the cold state (see, e.g., Lasota 2001; King et al. 2007).

The central accretion rate during a burst is determined by the viscous evolution in the high-viscosity hot part of the disk because the cold part evolves at a relatively low rate. The analysis of the viscous evolution of X-ray novae during outbursts provides an estimate of the turbulent parameter α in the hot state. The size of the hot part of the disk depends on the radial temperature distribution, meanwhile the disk temperature depends on the viscous heating rate and the incident flux of central X-rays. Previously, Suleimanov et al. (2008) have analysed X-ray and optical light-curves of A 0620-00 (1975) and GS 1124-68 (1991), which have

* E-mail: galja@sai.msu.ru

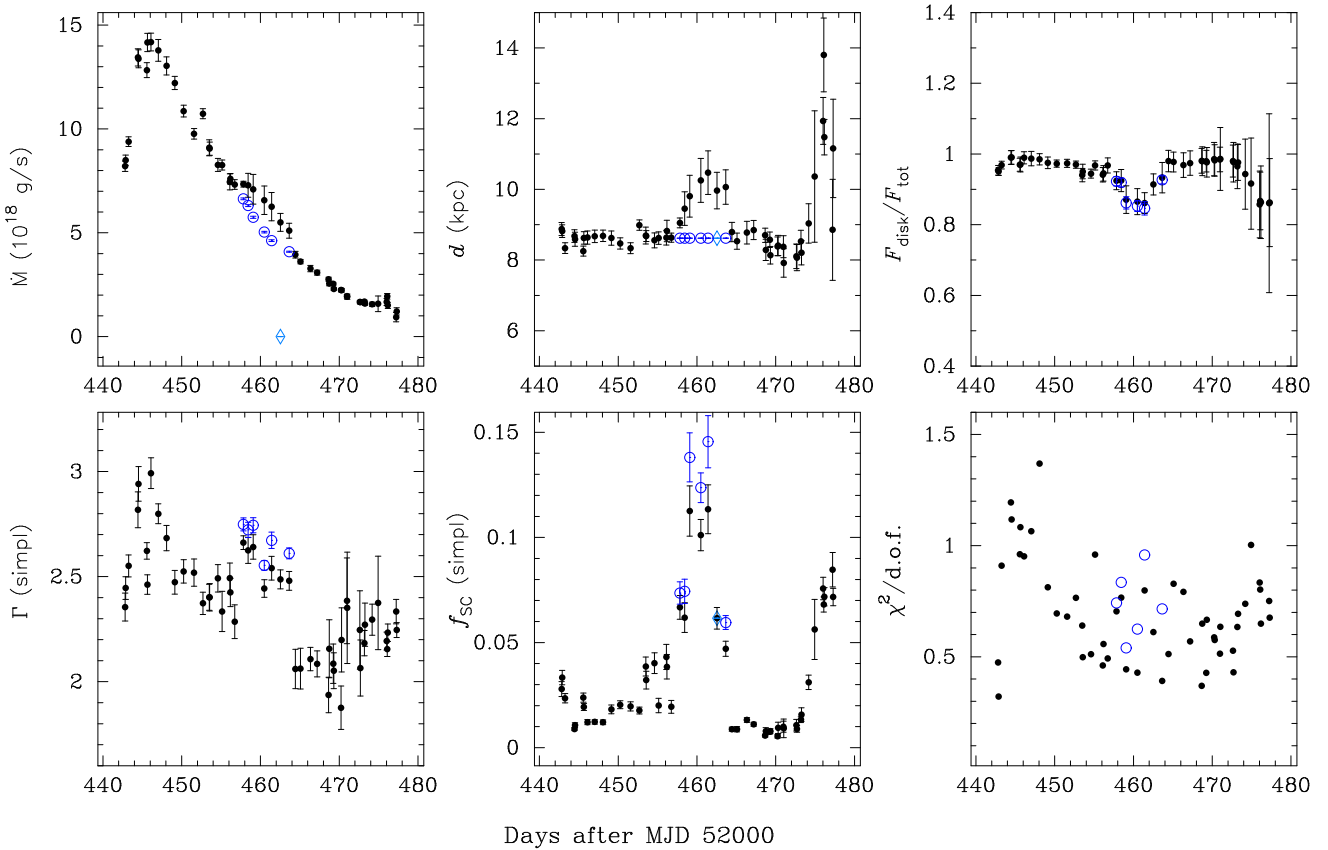


Figure 1. Evolution of spectral parameters \dot{M} , d , Γ and f_{sc} in XSPEC fits made with the model $tbabs * (simpl * kerrbb + laor) * smedge$ for the 2002 outburst of 4U 1543–47 observed by RXTE/PCA. The BH parameters are $m_x = 9.4$ and $a_{\text{Kerr}} = 0.4$, the disk inclination is $i = 20.7$. The left panels show the disk-to-total-flux ratio in 0.5 – 50 keV and reduced χ^2 . Empty circles denote the spectral fits made with the fixed distance ≈ 8.62 kpc, which has been found as the average for the observations at moments when the distance is least variable (before MJD 52456). The diamond stands for the spectral fit with a value of the reduced $\chi^2 > 2$.

fast-rise exponential-decay (FRED) X-ray light curves. They have considered the completely ionized disks with the fixed outer radius and obtained values of α depending on the black hole parameters (see also Malanchev & Shakura (2015)).

In the present work, we study details of the viscous evolution of the disk in X-ray transient 4U 1543–47 during the first ~ 30 days of the decay of its FRED-like outburst in 2002. The archival X-ray spectral observations by RXTE/PCA are used to derive the evolution of the central accretion rate $\dot{M}(t)$. System 4U 1543–47 (V* IL Lup) is a low mass X-ray binary (LMXB) that shows outbursts about every ten years. The compact accreting object is a reliable black hole (BH) candidate. The binary has an orbital period of 1.116 day (Orosz 2003), which is longer than those of most LMXBs with known orbital periods (Ritter & Kolb 2003). For example, the X-ray novae with BH candidates A 0620–00, GS 1124–68, GS 2000+25, and GRO 0422+32 have orbital periods less than 10 hours. The optical companion to 4U 1543–47 is an A2V star with a mass of $M_{\text{opt}} \sim 2.5 M_{\odot}$. The mass of the black hole has been estimated as $M_x = 2.7 - 7.5 M_{\odot}$ or $M_x = 9.4 \pm 2 M_{\odot}$, and the distance 9.1 ± 1.1 kpc (Orosz et al. 1998a, 2002). The latest observational result is a BH mass of $M_x = 8.4 - 10.4 M_{\odot}$ and an inclination of 20.7 ± 1.5 for the binary system (Orosz 2003).

Different scenarios or stages of the disk evolution during an outburst of an X-ray Nova are possible, which generally follow each other. During some time, the size of the hot zone can be constant, being approximately equal to the tidal truncation radius in the

binary system. In case of 4U 1543–47, this requires a strongly irradiated accretion disk. For less irradiated disk, the hot zone should be shrinking, although the irradiation may play an important role in the disk evolution. Finally, a stage of virtually negligible irradiation follows, resembling the disk decay in dwarf novae.

Using the observational data for 4U 1543–47, we study all these options. For a grid of the parameters m_x and a_{Kerr} , we compare the accretion rate $\dot{M}(t)$ obtained from the RXTE data with the theoretical results. The optical light curves in V and J bands obtained by Buxton & Bailyn (2004) are used to check the degree of self-irradiation. We assess the turbulent α -parameter in the hot state, as well as other disk properties of 4U 1543–47, and generalize our modelling results.

To model the evolution of a hot irradiated disk, 1-D code FREDDI has been developed and used in this work. The main input parameters of the code are as follows: the turbulent parameter α , the BH mass m_x ¹, and Kerr parameter a_{Kerr} . For a non-irradiated disk, we expect that a cooling front, which resembles that in a dwarf-nova disk, controls $\dot{M}(t)$ and the X-ray light curve. To model such evolution, we follow the approach used by Kotko & Lasota (2012) for normal outbursts of dwarf novae.

The structure of the paper is as follows. The spectral mod-

¹ We use two notations for the black hole mass: M_x is the mass in grams and $m_x = M_x/M_{\odot}$ is the mass in solar masses.

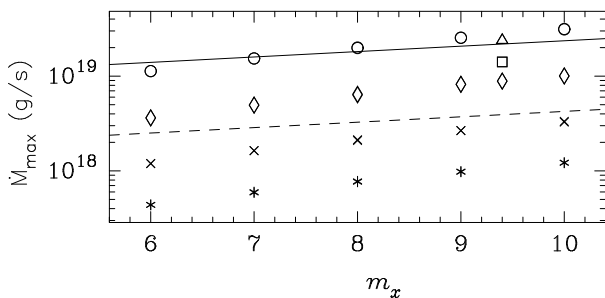


Figure 2. The modelled peak accretion rate of the 2002 outburst of 4U 1543–47 (at \sim MJD 52446) in different spectral models with $i = 20.7$ and $f_{\text{col}} = 1.7$ (see the caption of Table A1) versus the BH mass. The results for both spectral combinations are plotted, although the difference of their peak accretion rates is rather imperceptible. The symbols indicate the different values of a_{Kerr} : 0 (circles), 0.1 (triangle), 0.4 (square), 0.6 (diamonds), 0.9 (crosses), and 0.998 (asterisks). Two straight lines show the accretion rates corresponding to the Eddington limit L_{Edd} and different efficiencies of the accretion onto the black hole: for $a_{\text{Kerr}} = 0.0$ (solid) and $a_{\text{Kerr}} = 0.998$ (dashed). See Appendix A for details.

elling of RXTE archival data used to determine the accretion rate evolution is outlined in §2. In §3 we describe the ways of determining α for irradiated and non-irradiated disks. In §4 the modelled light curves and α are presented. The optical emission during the outburst is considered in §5. We discuss the self-irradiation of 4U 1543–47 and the model assumptions in §6 and give a summary in §7. All statistical errors in the work are the $1\text{-}\sigma$ confidence intervals.

2 SPECTRAL MODELLING OF THE ACCRETION RATE EVOLUTION OF 4U 1543–47 IN 2002

The outburst of 4U 1543–47 in 2002 had a FRED-like X-ray light curve with the first minor X-ray/IR re-flare at \sim 15 day and the second bigger IR/optical re-flare at \sim 40 day from the peak (Park et al. 2004; Buxton & Bailyn 2004). We analyse the same data obtained with the Proportional Counter Array aboard the *RXTE* observatory as in Park et al. (2004).

There are two main spectral components in the 4U 1543–47 burst spectra, as found by Park et al. (2004): the multicolour blackbody-disk thermal emission with a maximum around 1 keV and the non-thermal component at higher energies. To describe the thermal emission of the disk, Park et al. (2004) used the *diskbb* model as a spectral component in XSPEC (Arnaud 1996). In this model, parameter T_{in} , the ‘inner’ disk temperature, is an indicator of the accretion rate through the inner edge of the disk. An actual value of the accretion rate is related to T_{in} in a complex way because of the general relativity effects.

We use the *kerrbb* spectral model (Li et al. 2005) in XSPEC that takes into account general relativity effects on flux production and propagation of photons in the vicinity of a black hole, with \dot{M} as a free parameter. Here we outline the principle features of our modelling, and the details can be found in Appendix A.

The *kerrbb* parameters, which we set free, are the accretion rate \dot{M} and the distance d . For each fit, we fix the BH mass M_x and the dimensionless Kerr parameter a_{Kerr} . The disk inclination is the binary orbit inclination, 20.7 (Orosz 2003), or, alternatively, 32° (a value suggested by spectral modelling; Morningstar & Miller 2014). The list of these and other parameters can be found in Table A1 in Appendix A.

To describe the non-thermal component as the thermal emission comptonized by the high-temperature plasma near the disk, we use the convolution model *simpl* (Steiner et al. 2009) or the additive model *comptt* (Titarchuk 1994). Thus, two combinations of spectral components are used, including either *simpl* or *comptt*. As we have found, both spectral combinations give very similar peak magnitudes of \dot{M} .

For each spectral combination, we have obtained at least 20 accretion rate curves: for each pair of values of the BH mass and the Kerr parameter. An example of the evolution of some spectral parameters is shown in Fig. 1, where we adopt observationally suggested (hereafter ‘central’) disk parameters: $m_x = 9.4$, $a = 0.4$, $i = 20.7$ (Orosz 2003).

The peak accretion rates versus the BH parameters are shown in Fig. 2. The higher a_{Kerr} , the less the accretion rate is needed to generate the observed X-ray flux. The obtained accretion peak rates for $a_{\text{Kerr}} = 0$ are very close to the critical Eddington rate calculated as $L_{\text{Edd}}/(\eta(a_{\text{Kerr}})c^2) = (4\pi G M_x m_p)/(c\sigma_T \eta(a_{\text{Kerr}}))$, where $\eta(a_{\text{Kerr}})$ is the accretion efficiency. Above the limit, the standard thin disk model is inaccurate. However, we neglect this possibility in the present study, regarding the limit as a formal approximate value, meanwhile the excess is quite small.

For the observations around MJD 52460, when the accretion rate curve shows a bump (see the top left panel of Fig. 1), we have made additional spectral fits, fixing the distance at its average value (it is found as the average from the spectral fit results before MJD 52456 if $\chi^2 < 2$). The additional fits demonstrate that, apparently, the accretion rate decays smoothly (empty circles in Fig. 1). The bump on the $\dot{M}(t)$ curve (solid circles around MJD 52460) is probably a result of strong variations of the non-thermal component, or a manifestation of an extra spectral component, which cannot be properly described by the presumed spectral model.

3 DETERMINATION OF THE VALUE OF α FROM X-RAY NOVA OUTBURSTS

The viscous evolution of an accretion disk involves the radial redistribution of the viscous torque and the mass density. This process is described by the equation of diffusion type:

$$\frac{\partial \Sigma}{\partial t} = \frac{1}{4\pi} \frac{(GM_x)^2}{h^3} \frac{\partial^2 F}{\partial h^2}, \quad (1)$$

where $h \equiv \sqrt{GM_x r}$ is the specific angular momentum, Σ is the surface density, $F = 2\pi W_{r\varphi} r^2$ is the viscous torque expressed using the height-integrated viscous stress tensor $W_{r\varphi}$ (see, e.g. Lyubarskij & Shakura 1987). The viscous torque and surface density in the Keplerian disk are related as follows:

$$F = 3\pi h \nu_1 \Sigma, \quad (2)$$

where ν_1 is the kinematic coefficient of turbulent viscosity.

Using $F(h)$ as a radial characteristic is very effective. First, boundary conditions are usually set on F or its first derivative $\partial F/\partial h = \dot{M}$. Second, the viscous heating in the disk is explicitly related to the viscous torque, $Q_{\text{vis}} = 3(GM_x)^4 F/(8\pi h^7)$, and this relation holds for cases with $\dot{M} = 0$ too.

To illustrate how the viscous torque behaves, we plot schematically the $F(h)$ -distribution in the disk with the hot inner and cold outer parts (Fig. 3). At the inner boundary of the disk around the black hole, the viscous torque is zero: $F_{\text{in}} = 0$. A positive slope corresponds to mass inflow and vice versa. In the outer, cold neutral disk, the viscous torque is depressed. Between the cold and hot

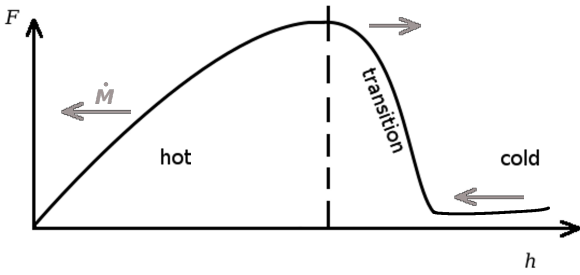


Figure 3. A schematic representation of the viscous torque distribution in the disk, which has the hot inner and cold outer zone. The grey arrows show the direction of the mass flow, and their heights indicate the representative moduli of the accretion rate. The slope of the curve $F(h)$ equals the accretion rate. In the outer cold disk, the accretion rate is suppressed due to a lower value of the kinematic coefficient of turbulent viscosity. There are two locations where the accretion rate $\dot{M} = \partial F/\partial h$ becomes zero.

zone, where the hydrogen undergoes recombination/ionization, the opacity coefficient varies strongly. If the disk in a binary system is fully ionized during some period of time, the outer radius of the disk may be considered stationary, corresponding to the dashed line (the corresponding quasi-stationary distribution of F is derived by Lipunova & Shakura 2000). The mass is lost from the disk through its inner boundary. When the accretion rate drops to such level that the surface density in the hot disk becomes less than a critical value, the outside-in transition to the cold state begins (Smak 1984b).

At the outer boundary of the hot zone (the dashed line in Fig. 3), the viscous torque F reaches an extremum. Subsequently, we assume that the mass flow becomes zero at the boundary: $\partial F/\partial h = 0$. There is a mass outflow in the transition zone, and the mass accumulates in the cold zone while the transition region moves towards the centre. In the cold zone, it takes a longer time for a quasi-stationary distribution to develop, hence, the slope of $F(h)$ is not constant there.

There are three successive stages of an outburst decay in X-ray novae as suggested by Dubus et al. (2001): (1) the hot zone has the constant radius R_{hot} due to the strong irradiation (this stage can be absent if the disk is too large); (2) the cooling front begins to move, its position being determined by the irradiation; (3) the cooling front propagates with the speed $\sim \alpha_{\text{hot}} u_{\text{sound}}$, when the irradiation is not important. Two first stages are possible only if the irradiation is strong enough. Fig. 3 qualitatively describes each of these three stages. In the three following subsections, we describe methods to model these stages.

3.1 The hot disk with a fixed outer radius

If the outer radius is constant, the e -folding time of the accretion rate viscous decay in the disk around a stellar-mass black hole in a binary system is

$$t_{\text{exp}} \approx 0.45 R_{\text{out}}^2 / \nu_t(R_{\text{out}}) \quad (3)$$

The above relation is obtained as an approximation of the exact solution for evolution of the disk whose kinematic viscosity $\nu_t(r)$ does not change with time (Lipunova 2015). Such a viscous disk with the fixed outer radius yields a precisely exponential decay of $\dot{M}(t)$.

In α -disks (Shakura & Sunyaev 1973), the kinematic coefficient of turbulent viscosity depends on the surface density and, respectively, on time: $\nu_t = \nu_t(r, t)$. The solution for the decay of a hot α -disk with a fixed outer radius has been found by Lipunova

& Shakura (2000). The accretion rate decays as $\dot{M} \propto t^{-10/3}$ in the regime of the Kramers opacity. Such a steep decay can be observed in X-rays as an exponential decay.

The analytic solution may be applied for a time interval when the whole disk is in the hot state. This can happen due to a high viscous heating or a strong irradiating flux, keeping the whole disk in the completely ionized state. (King & Ritter 1998; Shahbaz et al. 1998; Esin et al. 2000; Dubus et al. 2001, also Meyer & Meyer-Hofmeister (1984, 1990)). Ertan & Alpar (2002) have suggested that the radius R_{hot} may be constant, although smaller than the disk size, if a specific height profile is developed with a stationary boundary between the hot and cold zone, beyond which the disk is shadowed from the central X-rays.

One can estimate α using (3). Let us parametrize the local viscous stress tensor in the equatorial plane of the disk as $w_{r\phi} = \alpha P_c$, where P_c is the total pressure (Shakura & Sunyaev 1973). For the outer parts of the hot disk, the gas pressure dominates. On the other hand, $w_{r\phi} = \frac{3}{2} \omega_K \nu_t \rho_c$ (c.f. Eq. (2)). Substituting $P_c/\rho_c = \mathfrak{R} T_c/\mu$ yields a relation between ν_t and α : $\nu_t = \frac{2}{3} (\alpha/\omega_K) (\mathfrak{R} T_c/\mu)$. Following the work of Ketsaris & Shakura (1998), we use the relation between T_c and the half-thickness z_0 , which is the depth where the optical thickness $\tau = 2/3$ and $T = T_{\text{eff}}$: $\mathfrak{R} T_c/\mu = \omega_K^2 z_0^2/\Pi_1$; Π_1 is a dimensionless parameter depending on the total optical thickness of the disk in the vertical direction; it has been calculated by Ketsaris & Shakura (1998) and Malanchev et al. (2017). We arrive at the relation $\nu_t(r) = \frac{2}{3} (\alpha/\omega_K) (\omega_K^2 z_0^2/\Pi_1)$ and, hence,

$$\alpha \sim 0.15 \left(\frac{R_{\text{out}}}{2 R_{\odot}} \right)^{3/2} \left(\frac{z_0/R_{\text{out}}}{0.05} \right)^{-2} \left(\frac{M_x}{10 M_{\odot}} \right)^{-1/2} \left(\frac{t_{\text{exp}}}{30 \text{d}} \right)^{-1} \times \Pi_1, \quad (4)$$

where t_{exp} is the e -folding of the accretion rate decay, z_0 is the disk half-thickness near the outer radius, and $\Pi_1 = 5.5 - 6$. To estimate α , one should substitute z_0 corresponding to the peak of an X-ray nova outburst.

The main uncertainty in the above formula is the radius of the disk. In addition, the evolution of the half-height of the α -disk leads to a variation of the numerical factor in (4). However, the modelling of the disk evolution can provide a self-consistent value of α . This was done for outbursts of A 0620–00 (1975) and GS 1124–68 (1991) by Suleimanov et al. (2008). Using our code FREDDI², we find that for any fully-ionized viscously-evolving accretion disk

$$\alpha \approx 0.21 \left(\frac{R_{\text{hot}}}{R_{\odot}} \right)^{25/16} \left(\frac{t_{\text{exp}}}{30 \text{d}} \right)^{-5/4} \left(\frac{\dot{M}_{\text{max}}}{10^{18} \text{ g s}^{-1}} \right)^{-3/8} m_x^{5/16}, \quad (5)$$

for the Kramers opacity, or

$$\alpha \approx 0.20 \left(\frac{R_{\text{hot}}}{R_{\odot}} \right)^{12/7} \left(\frac{t_{\text{exp}}}{30 \text{d}} \right)^{-9/7} \left(\frac{\dot{M}_{\text{max}}}{10^{18} \text{ g s}^{-1}} \right)^{-3/7} m_x^{2/7} \quad (6)$$

for the OPAL approximation. Power indexes in the above expressions are obtained when substituting the thickness of the disk in (4) by its analytic expression from Suleimanov et al. (2007). An accuracy of the numerical factors is 5%. Details of the FREDDI code can be found in Appendix B.

Let us estimate α for 4U 1543–47, supposing that the fast viscous evolution has swept the whole disk. The Roche lobe effective radius of the primary in 4U 1543–47 is $R_{\text{RL}} \approx 4.2 - 5.3 R_{\odot}$ (Eggleton 1983) for the BH mass lying in the interval $M_x = 6 - 10 M_{\odot}$. The maximum disk radius in 4U 1543–47 can be as large as $\sim 4 R_{\odot}$, if the tidal interactions with the companion truncate the disk at

² FREDDI can be freely downloaded from the authors' web page <http://xray.sai.msu.ru/~malanchev/freddi/>.

$R_{\text{id}} \approx 0.8 R_{\text{RL}}$ (Paczynski 1977; Suleimanov et al. 2007). When substituting the radius and other parameters for 4U 1543–47 in (5) or (6), namely, $t_{\text{exp}} = 15^{\text{d}}$, $m_x = 9.4$, $\dot{M}_{\text{max}} = 1.4 \times 10^{19}$ g/s (from Fig. 1, the upper left panel), we obtain $\alpha \sim 3.2 - 3.3$, an unphysical value. This result indicates that the disk evolved in a different manner. Most probably, during the burst of 2002 the outer parts of the disk in 4U 1543–47 remained cold.

3.2 Disks with R_{hot} controlled by irradiation

After the recombination starts, the radius of the hot disk decreases. If the X-ray heating is strong, the radius of the hot zone R_{hot} is determined by the incident flux, that is, by the central accretion rate. Dubus et al. (2001) argue that the transition between the hot and cold portions of the disk in X-ray transients is determined by the position where $T_{\text{irr}} = 10^4$ K. This is explained by the fact that the cold state exists only for lower T_{eff} (Meyer & Meyer-Hofmeister 1984; Tuchman et al. 1990). Some evidence for such behaviour was found by Hynes et al. (2002) in the 1999 – 2000 outburst of XTE J1859+226, although they suggested that the condition at the hot zone radius R_{hot} may be more complex.

We adopt the following parametrization for the flux irradiating the outer disk (Lyutyi & Sunyaev 1976; Cunningham 1976):

$$Q_{\text{irr}} \equiv \sigma_{\text{SB}} T_{\text{irr}}^4 = C_{\text{irr}} \frac{L_{\text{bol}}}{4\pi r^2}, \quad (7)$$

where $L_{\text{bol}} = \eta(a_{\text{Kerr}}) \dot{M} c^2$ is the bolometric flux, $\eta(a_{\text{Kerr}})$ is the accretion efficiency, σ_{SB} is the Stephan–Boltzmann constant, and C_{irr} is the irradiation parameter. We assume in the present study that $C_{\text{irr}} = \text{const}$ (see discussion in §6.1).

We calculate the radius of the hot zone $R_{\text{hot}}(t)$ from

$$\sigma T_{\text{hot}}^4 = C_{\text{irr}} \frac{\eta(a_{\text{Kerr}}) \dot{M}_{\text{in}}(t) c^2}{4\pi R_{\text{hot}}(t)^2}, \quad (8)$$

where $T_{\text{hot}} = 10^4$ K and $\dot{M}_{\text{in}}(t)$ is the accretion rate through the inner edge of the disk.

In Fig. 4, we show the hot zone size versus the BH mass for 4U 1543–47, calculated for two different irradiation factors: $C_{\text{irr}} = 5 \times 10^{-3}$ (the value suggested for X-ray novae (Dubus et al. 2001)) and $C_{\text{irr}} = 5 \times 10^{-4}$. The black symbols for R_{hot} correspond to the peak accretion rate (MJD 25446) and the green symbols on-line represent the accretion rate at the end of the studied interval (MJD 52474).

When the accretion rate is high and $R_{\text{hot}}(\dot{M}) > R_{\text{id}}$, the hot zone extends through the entire disk and, hence, the viscously evolving region has a constant radius. As we can see from Fig. 4 for $C_{\text{irr}} = 5 \times 10^{-3}$ (top), the whole disk would have been hot during almost entire investigated time interval. For lower C_{irr} , the hot zone radius becomes smaller than R_{id} (see Fig. 4, the lower panel) and cannot be constant during the investigated time interval.

The relative importance of the irradiation comparing to the viscous heating can be expressed as follows:

$$\frac{Q_{\text{irr}}}{Q_{\text{vis}}} = \frac{4}{3} \eta(a_{\text{Kerr}}) C_{\text{irr}} \frac{r}{R_{\text{grav}}} \frac{1}{f_F(r)} \quad (9)$$

(e.g. Suleimanov et al. 2007), where $R_{\text{grav}} = 2G M_x/c^2$ and the viscous heating

$$Q_{\text{vis}} = \frac{3}{8} \frac{\sqrt{GM_x}}{\pi} \frac{F}{r^{7/2}}, \quad F = \dot{M}_{\text{in}} h f_F(r). \quad (10)$$

For the quasi-stationary solution of Eq. (1), the dimensionless factor $f_F(r) \approx 0.7$ at the radius where $\dot{M} = 0$ (Lipunova & Shakura

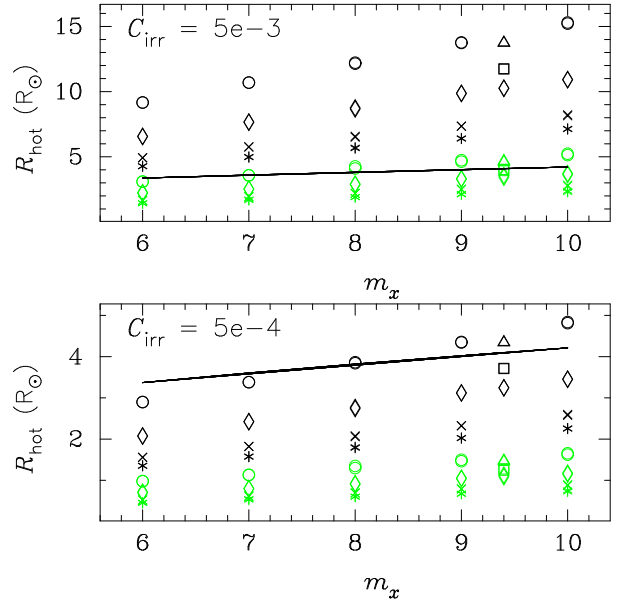


Figure 4. The hot-zone radius ($T_{\text{irr}} = 10^4$ K) as a function of BH mass at the accretion peak on MJD 25446 (black symbols), and at the end of the investigated light curve, MJD 25474 (green symbols on-line). $C_{\text{irr}} = 5 \times 10^{-3}$ in the top panel, and $C_{\text{irr}} = 5 \times 10^{-4}$ in the lower panel. Symbols have the same meaning as in Fig. 2, which shows the corresponding peak accretion rates. Solid line is the tidal radius of the accretion disk, which is a function of the central mass.

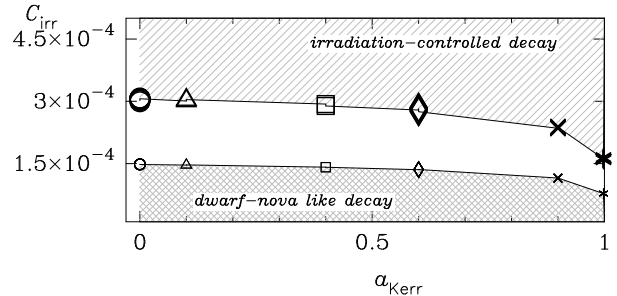


Figure 5. Critical values of C_{irr} , determining the type of hot disk evolution in 4U 1543–47 during the 2002 burst, versus the Kerr parameter. The points of the lower sequence (small symbols) represent the boundary below which the irradiation is so low that it cannot influence the hot zone size, and the cooling front propagates like in a normal outburst of a dwarf nova. Such C_{irr} are obtained from $Q_{\text{irr}}/Q_{\text{vis}}(R_{\text{hot}}) = 1$ at the burst peak. The big symbols in the higher sequence represent the values of C_{irr} , above which the whole modelled light curve should be explained by evolution of the irradiated hot zone, following the equation $Q_{\text{irr}}/Q_{\text{vis}}(R_{\text{hot}}) = 1$ at the end of the studied time interval. The symbols are of the same meaning as in Fig. 2. There is no dependence on m_x .

2000). The ratio (9) does not depend on the accretion rate in the approximation of constant C_{irr} . The illumination is more important for bigger disks. If $Q_{\text{irr}} > Q_{\text{vis}}$ at R_{hot} , a change in $R_{\text{hot}}(t)$ is determined by a variation of the irradiating flux. As the latter depends on $\dot{M}(t)$, the radius of the hot zone shifts at a rate determined by the viscous timescale at R_{hot} .

Fig. 5 presents values of C_{irr} , critical in the context of explaining the decay of 2002 burst of 4U 1543–47. The higher sequence of symbols represents the minimum values of C_{irr} above which the whole modelled light curve should be explained by the irradiation-

controlled hot zone. These values are found from the condition $Q_{\text{irr}}/Q_{\text{vis}} = 1$ at R_{hot} at the end of the studied time interval, taking into account Eq. (8).

To model evolution of the irradiation-controlled hot disk, we solve the viscous diffusion equation (1) on the interval from R_{in} to R_{hot} using our FREDDI code. The condition $\dot{M} = 0$ is set at R_{hot} . The outer boundary thus corresponds to the vertical dashed line in Fig. 3. Physically, the transition to the cold disk starts there, so we determine R_{hot} at each step using (8).

All models, calculated by FREDDI for the present study, are obtained with the quasi-stationary distribution as the initial one. This corresponds to the calculation of the decaying part of the burst, although FREDDI can simulate the light curve from the early rise (see Appendix B).

3.3 Cooling front without irradiation

If X-ray heating is very low, a so-called cooling front, surrounding the hot zone, propagates towards the centre while the accretion rate decreases. The heating and cooling fronts without irradiation have been studied to explain dwarf nova bursts (Hōshi 1979; Meyer & Meyer-Hofmeister 1981; Smak 1984a; Meyer 1984; Lin et al. 1985; Cannizzo 1994; Vishniac & Wheeler 1996; Menou et al. 1999; Smak 2000).

Numerical modelling of DIM in dwarf novae shows that, if α_{hot} is constant, the speed of the cooling front approaches a characteristic constant velocity of order of $\alpha_{\text{hot}} u_{\text{sound}}$ (Meyer 1984; Cannizzo 1994; Vishniac & Wheeler 1996), with the hot inner part of the disk evolving in a self-similar way (Menou et al. 1999).

Using analytic approximations to numerical results of DIM, Kotko & Lasota (2012) considered about 20 outbursts of dwarf novae and AM CVn stars to determine the hot disk viscosity parameter α_{hot} from the measured decay times. This method relies on the implied velocity of the cooling front propagation. Kotko & Lasota (2012) have also used the DIM, which is able to reproduce the normal outbursts of dwarf novae, in order to relate the amplitudes of the outbursts and the recurrence times. Both methods yield $\alpha_{\text{hot}} \sim 0.1 - 0.2$.

Similarly, to reproduce the light curve of 4U 1543–47 in the model of the cooling front propagation without irradiation, we adopt the approximations to numerical modelling by Menou et al. (1999). The accretion rate decays as

$$\dot{M}(t) = \dot{M}_{\text{peak}} (R_{\text{front}}(t)/R_{\text{hot,peak}})^{2.2}, \quad (11)$$

where the radius of the hot zone

$$R_{\text{front}}(t) = R_{\text{hot,peak}} - u_{\text{front}} t$$

can be found using the front velocity

$$u_{\text{front}} = k \alpha u_{\text{sound}}, \quad u_{\text{sound}} = \sqrt{\mathcal{R} T_{\text{crit}}/\mu}, \quad k \approx 1/14. \quad (12)$$

At the front, the disk temperature at the central plane is $T_{\text{crit}} = 4.7 \times 10^4$ K (Kotko & Lasota 2012) and the molecular weight $\mu = 0.6$. Since irradiation is not important, the maximum radius of the hot disk is found from the rate of the viscous heating (10) at the peak:

$$Q_{\text{vis}}(R_{\text{hot,peak}}) = \sigma_{\text{SB}} T_{\text{hot}}^4, \quad T_{\text{hot}} = 10^4 \text{ K}. \quad (13)$$

As can be seen from Fig. 5, the above approach is appropriate for 4U 1543–47 (2002) if $C_{\text{irr}} \lesssim 1.5 \times 10^{-4}$. The low set of symbols in Fig. 5 represents the critical values of the irradiation parameter C_{irr} for 4U 1543–47 in 2002, below which the self-irradiation could not control the disk evolution. The values are obtained from

the condition that $Q_{\text{irr}}/Q_{\text{vis}}(R_{\text{hot}}) = 1$ at the burst peak, taking into account Eq. (8). Since ratio (9) decreases with the radius, the effect of irradiation becomes only less during the decay as R_{hot} decreases.

By applying the approximation of the constant-speed cooling front, α may be expressed as follows:

$$\alpha_{\text{hot}} \approx 0.16 \frac{R_{\text{hot}}^{\text{max}}}{R_{\odot}} \left(\frac{t_{\text{exp}}}{10^{\text{d}}} \right)^{-1} \left(\frac{k}{1/14} \right)^{-1} \left(\frac{u_{\text{sound}}}{25 \text{ km s}^{-1}} \right)^{-1}. \quad (14)$$

Expressing the hot-zone size at the peak $R_{\text{hot}}^{\text{max}}$ from the accretion rate \dot{M}_{max} using (13), we rewrite the last relation as:

$$\alpha_{\text{hot}} \approx 0.07 \left(\frac{m_{\text{x}} \dot{M}_{\text{max}}}{10^{18} \text{ g s}^{-1}} \right)^{1/3} \left(\frac{10^{\text{d}}}{t_{\text{exp}}} \right) \left(\frac{10^4 \text{ K}}{T_{\text{hot}}} \right)^{4/3} \left(\frac{1/14}{k} \right) \left(\frac{25 \text{ km s}^{-1}}{u_{\text{sound}}} \right). \quad (15)$$

The numerical factor in (15) depends on the power-law index of $\dot{M}(R_{\text{hot}})$ in relationship (11).

4 RESULTS OF FITTING OF THE ACCRETION-RATE EVOLUTION FOR 4U 1543–47 (2002)

4.1 Mild irradiation

The viscous evolution of the hot part of the disk whose size is controlled by irradiation (§3.2) can explain the shape of the observed curve $\dot{M}(t)$. For characteristic values of C_{irr} shown in Fig. 5 (the upper boundary between the empty and shaded areas, $C_{\text{irr}} = (2-3) \times 10^{-4}$), we solve equation (1) numerically using code FREDDI to find $\dot{M}(t)$. Comparing it with $\dot{M}(t)$ derived from the spectral modelling (see § 2), we find the best-fit values of α for a grid of BH parameters (Fig. 6).

Higher values of C_{irr} would correspond to larger hot-zone size R_{hot} , according to (8). Since the observed t_{exp} is fixed, this would require bigger values of α .

An example of a model with the minimal χ^2 statistic is presented in Fig. 7. The top panel shows the evolution of the rate of accretion through the inner radius for the parameters indicated in the plot, along with the spectral-modelling results from Fig. 1. In the lower panel of Fig. 7, the evolution of the irradiation-controlled hot-zone size is shown for the same parameters by black. By green and red (online), we show the hot-zone radius evolution for two other sets of parameters, representing extreme cases within the parameters' limits considered. Values of the accretion rate and distance to the source are unique for each set.

Values of α , found by FREDDI for such scenario, lie in the interval $\sim 0.5 - 1.5$ (see Fig. 6). It is possible that FREDDI does not fully account for complex effects appearing when the outer boundary R_{hot} is moving. This can bias the resulting α towards bigger values. We discuss this further in §6.2. The results, presented in Fig. 6, can be approximated in a way similar to (5) or (6). The approximation has the same power indexes from the disk parameters, while the dimensionless numerical factor is less: 0.17, for Kramers opacity, and 0.15, for OPAL approximation, with an accuracy of $\sim 12\%$.

If C_{irr} lied in the interval $(1.5 - 3) \times 10^{-4}$, it would follow from the picture described in §3.2 and 3.3, that the cooling front of ‘dwarf-nova-disk’ type had started sometime during the investigated time interval. A visible change in the evolution of $\dot{M}(t)$ is expected, when irradiation fails to support the outer hot disk (Dubus et al. 2001), but further modelling is needed to study this in detail. Notice that there are no suspicious turns in the $\dot{M}(t)$ curve during MJD 25446–25474 (see the note at the end of §2).

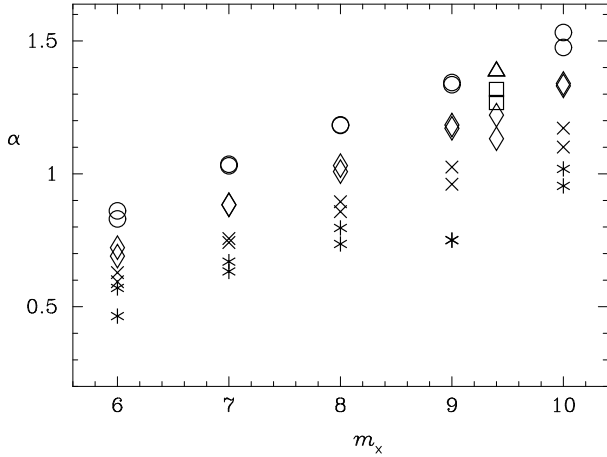


Figure 6. The α -parameter, which the ionized disk in 4U 1543–47 (2002) had, if its size was controlled by irradiation (§3.2). Values of α are obtained for values of C_{irr} shown in Fig. 5 by bigger symbols. Each value of α is obtained using χ^2 minimization of the $\dot{M}(t)$ curve. The radius of the hot zone corresponds to $T_{\text{irr}} = 10^4$ K. As before, the symbols indicate different values of a_{Kerr} : 0 (circles), 0.1 (triangle), 0.4 (square), 0.6 (diamonds), 0.9 (crosses), and 0.998 (asterisks). Each pair of parameters (m_x, a_{Kerr}) has two resulting α for two XSPEC models, with either *simple* or *comptt* component.

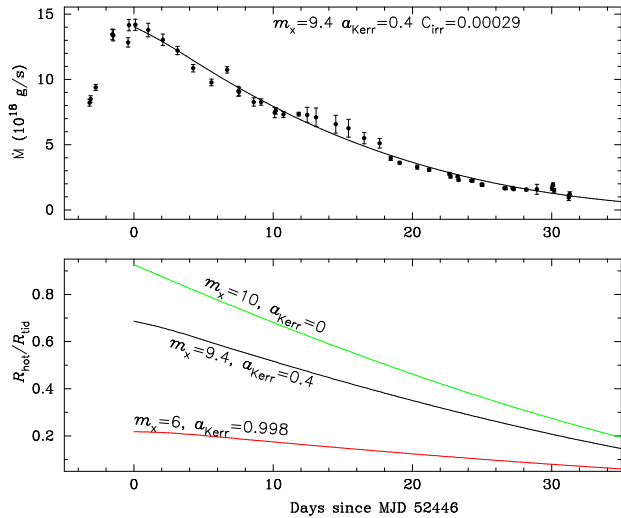


Figure 7. The model of a hot zone controlled by irradiation. The top panel: modelled and observed $\dot{M}(t)$ of 4U 1543–47 (2002) for the set of parameters indicated on the plot. The lower panel: the evolution of the hot-zone radius R_{hot} in units of the tidal radius R_{tid} : the black curve is the model from the top panel; the green and red curves are extreme cases with the parameters indicated. The tidal radius R_{tid} depends on m_x (see Fig. 4).

4.2 No irradiation

For $C_{\text{irr}} \lesssim 1.5 \times 10^{-4}$, we can describe the burst decay using the same approach as used for normal outbursts of dwarf novae (see §3.3). For the cooling front moving with a constant speed and the peak radius of the hot zone corresponding to $T_{\text{hot}} = 10^4$ K, we obtain α shown in Fig. 8 for the same grid of the values m_x and a_{Kerr} . All values of α are in the interval 0.08 – 0.32.

Fig. 9 shows the modelled accretion rate for the specific BH parameters: $m_x = 9.4$ and $a_{\text{Kerr}} = 0.4$ (the top panel). The lower panel of Fig. 9 shows the hot-zone radius evolution for three sets of

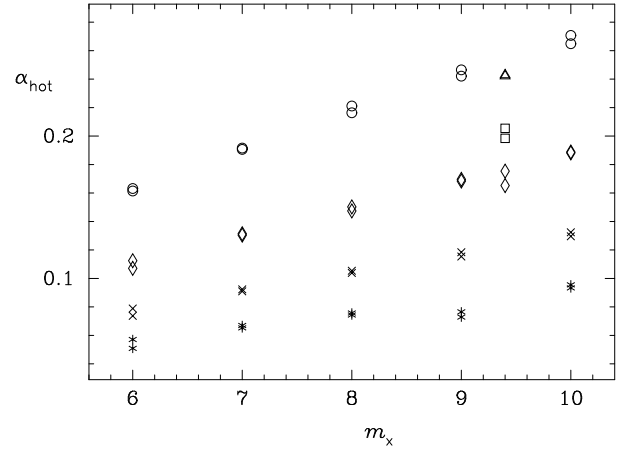


Figure 8. The best-fit α obtained for the burst of 4U 1543–47 (2002) in the approximate cooling-front model (Menou et al. 1999). The accretion rate evolves in accordance with the expressions in §3.3. Different symbols indicate values of a_{Kerr} as in Fig. 6.

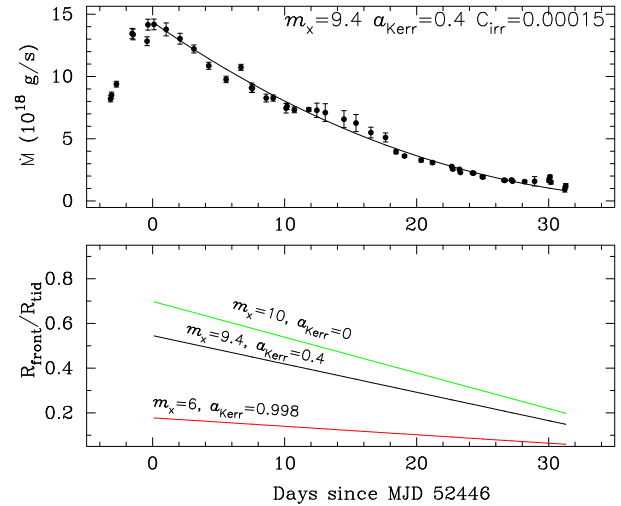


Figure 9. The model of the cooling front propagating with a constant speed without irradiation. Top panel: evolution of $\dot{M}(t)$ for parameters $\alpha_{\text{hot}} = 0.23$, $m_x = 9.4$, $a_{\text{Kerr}} = 0.4$. Lower panel: the radius of the hot zone for these (black) and other parameters (green and red, online).

the parameters. As can be seen from the comparison of Figs. 7 and 9, the hot-zone radius is less for the no-irradiation scenario for the same disk parameters. The smaller size of the hot disk is one of the reasons for lesser values of α . Notice that the optical observations could be used to constrain the radius of the hot disk.

5 OPTICAL EMISSION FROM THE DISK IN 4U 1543–47 (2002)

Last decade studies have provided evidence that the optical emission during an X-ray Nova outburst could be produced not only by the outer parts of the disk illuminated with the central radiation. The low-frequency portion of the non-thermal emission from the BH vicinity can contribute to optical flux. Studies of correlation between X-ray, optical, infrared, and radio emission of some X-ray transients suggest that jets are responsible for at least a part of the emission (e.g., Russell et al. 2006; Rahoui et al. 2011). Non-

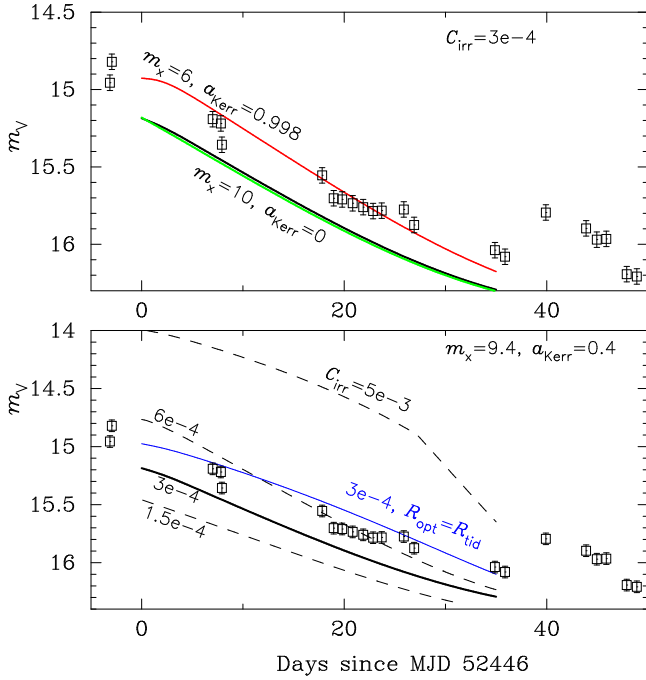


Figure 10. Observed and modelled optical V light curves of 4U 1543–47. The model flux is produced by the hot zone and calculated using observed $\dot{M}(t)$. The interstellar extinction and pre-burst flux are included. Observational points are the ISM-reddened data from Buxton & Bailyn (2004). The top panel shows models with $C_{irr} = 3 \times 10^{-4}$ and extreme values of the BH parameters, indicated near the curves (red and green line). The bold black curve (close to the lowest green line in the top panel) is obtained for $C_{irr} = 3 \times 10^{-4}$, $m_x = 9.4$ and $\alpha_{Kerr} = 0.4$. In the lower panel, modelled light curves are presented for fixed BH parameters and different values of C_{irr} . The higher solid curve (blue online) is the flux produced by the disk with constant size equal to the tidal radius.

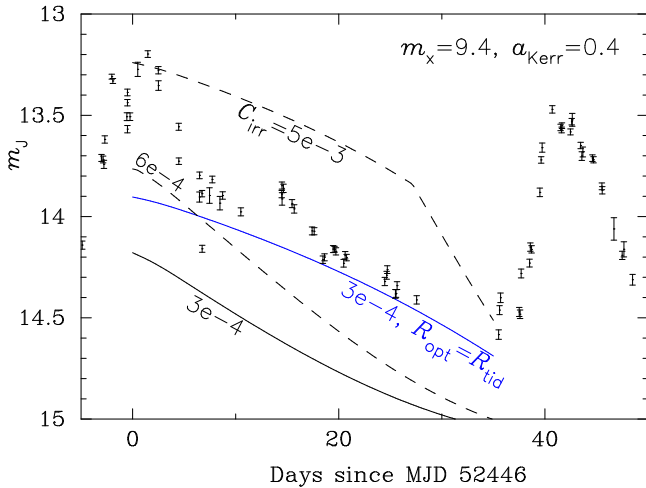


Figure 11. Same as the lower panel of Fig. 10 but for the J optical band.

thermal electrons in the central disk corona can produce power-law OIR spectra (the hybrid hot-flow model; see Poutanen & Veledina (2014)).

Here we consider the optical emission only from the accretion disk. Figs. 10 and 11 present a comparison of the modelled optical light curves with the data of Buxton & Bailyn (2004). If not stated otherwise, the optical flux is integrated only from the hot part of the multi-colour disk using $\dot{M}(t)$ derived from the spectral modelling. The effective temperature of a disk ring is calculated as $T_{eff}^4 = (Q_{irr} + Q_{vis})/\sigma$.

The modelled optical flux depends on the irradiation parameter C_{irr} , BH mass and Kerr parameter (because the mass and accretion efficiency affect derived \dot{M}), and hot-zone radius. The hot-zone radius itself depends on C_{irr} via (8) or on α via (12). It is important to note that a value of the turbulent parameter α , derived in the previous section, is a dynamical characteristic of the disk and depends on C_{irr} but does not affect directly the observed optical flux in the case of the irradiation-controlled hot zone.

The V and J optical bands are chosen because there are data in these bands just before the onset of the burst. Spectral flux densities at $\lambda_V = 5500 \text{ \AA}$ and $\lambda_J = 12600 \text{ \AA}$ are converted to the optical V and J magnitudes using the zero-fluxes $F_V^0 = 3.750 \times 10^{-9} \text{ erg s}^{-1} \text{ cm}^{-2} \text{ \AA}^{-1}$ and $F_J^0 = 3.021 \times 10^{-10} \text{ erg s}^{-1} \text{ cm}^{-2} \text{ \AA}^{-1}$ (Cox 2015). The optical interstellar extinction is accounted for in the plotted light curves as $A_V = 1.6 \text{ mag}$ (Orosz et al. 1998b) and $A_J = 0.282 A_V$ (Buxton & Bailyn 2004).

To plot the model curves, we add the modelled optical fluxes to the pre-burst flux, namely, 16.43 mag in V and 15.13 mag in J . The modelled magnitudes do not include a possible optical flux from other sources: due to reprocessed X-rays by the outer cold disk, companion star, jet, or corona. There is an exception though: we show the upper limit on the flux from the disk, calculated as if the accretion rate is uniform up to R_{tid} : the curves with the notation ‘ $R_{opt} = R_{tid}$ ’ in Figs. 10 and 11 (blue online).

Emission in the J band is much more variable than in V . Buxton & Bailyn (2004) have shown that the optical/IR spectrum at the secondary maximum arising ~ 40 days after the peak is explained by a jet (low-frequency power-law component in the spectrum). Other large J variations, visible before the 40th day, may also be associated with emission of this type.

Figures 10 and 11 demonstrate that the irradiation parameter $C_{irr} \sim 5 \times 10^{-3}$ is excluded, otherwise the optical flux from such a disk would greatly exceed the observed V and J values. From the V data alone, $C_{irr} \approx (3-6) \times 10^{-4}$ is suggested, taking into account possible extra emission from the irradiated outer cold disk. A value of C_{irr} deduced from the J data is approximately the same, although there is some uncertainty due to large flux variations in the J band. Very weak irradiation, $C_{irr} \approx 1.5 \times 10^{-4}$, needed to allow the dwarf-nova type evolution (§ 3.3), is less preferred from the point of view of optical observations but could not be excluded altogether in view of other possible sources of the optical photons.

6 DISCUSSION

6.1 Values of C_{irr}

There are several similar definitions of C_{irr} in the literature depending on how the central luminosity is expressed. Esin et al. (2000) have used the total X-ray luminosity obtained from analysing the X-ray data, and this C_{irr} is greater by a factor of L_{tot}/L_X than that defined by (7); Dubus et al. (1999) have expressed the irradiation

flux using $\dot{M} c^2$, which decreases C_{irr} by a factor of the accretion efficiency η . In (7) we follow [Dubus et al. \(2001\)](#) and [Suleimanov et al. \(2008\)](#), bearing in mind that L_{tot} does not depend on an observational band or inclination of a binary system. When trying to check the idea of C_{irr} being a universal value for X-ray transients, it's preferable to free oneself from additional biases. On the other hand, a large degree of uncertainty may be involved with the factor C_{irr} due to unknown geometry factors, albedo, and thermalization efficiency.

The irradiation parameter can be written as follows ([Suleimanov et al. 2007](#)):

$$C_{\text{irr}} = (1 - A_X) \Psi(\theta) \left(\frac{dz}{dr} - \frac{z}{r} \right), \quad (16)$$

where $\Psi(\theta)$ is the angular distribution of the central flux, z is the height of the interception of the central irradiation, θ is the polar angle of the vector from the disk centre to the intercepting unit surface. The term in the brackets determines the inclination of the illuminated surface to the incident radiation. Factor $1 - A_X$, equivalent to the 'thermalization coefficient', determines a portion of the intercepted bolometric flux that is absorbed and reprocessed to the black-body radiation. For the Newtonian metric and a flat disk, we have $\Psi(\theta) = 2 \cos(\theta) \approx 2z/r$. An inclusion of the general relativity effects modifies the angular distribution even for a non-rotating black hole. For an extremely fast rotating black hole, the angular distribution becomes remarkably flat (see figure 9 of [Suleimanov et al. 2007](#)). Here we assume that the disk is thin and the distance from the centre to the illuminated surface equals the cylindrical coordinate r .

Let us consider the case of the direct illumination of the α -disk surface. For a simple model of a central X-ray source with the geometry of a flat disk around a stellar-mass compact object ([Suleimanov et al. 2007](#)):

$$C_{\text{irr}} \sim 6 \times 10^{-5} \left(\frac{z_0/r}{0.05} \right)^2 \frac{1 - A_X}{0.1}. \quad (17)$$

Factor $1 - A_X$ depends on the disk albedo and spectral-dependent efficiency of reprocessing X-rays into thermal photons. The shape of an X-ray spectrum is important: mainly the relatively hard X-rays (> 3 keV) penetrate deep enough into the disk to be thermalized efficiently, and $1 - A_X \sim 0.05 - 0.1$ ([Suleimanov et al. 1999](#)). The formula above does not take into account the relativistic amplification due to the photon focusing. This amplification factor can reach 3–4 for a rapidly rotating Kerr black hole with $a_{\text{Kerr}} = 0.9981$ in the direction $\cos(\theta) = 0.1$ ([Suleimanov et al. 2007](#)).

Formula (17) demonstrates that generally C_{irr} is variable: the thermalization coefficient ($1 - A_X$) changes if the X-ray spectrum becomes softer, and the half-height z_0 of the disk gets smaller with decreasing accretion rate. Moreover, the magnitude of C_{irr} in (17) does not seem to be large enough to be able to explain the optical data of X-ray transients, even with relativistic effects taken into account ([Suleimanov et al. 2007](#)). Different ideas have been put forward to eliminate this discrepancy. For example, illumination through an inhomogeneous corona above the disk may yield a higher factor C_{irr} ([Suleimanov et al. 2003, 2007](#); [Gierliński et al. 2009](#)). [Suleimanov et al. \(2008\)](#) and [Mescheryakov et al. \(2011\)](#) have shown for some LMXBs that the effective geometric thickness can be twice as large as the hydrostatic thickness of the α -disk. On the other hand, according to [Dubus et al. \(1999\)](#), the cold disk may be shadowed by the hot disk from the central irradiation and, thus, factor C_{irr} in the cold disk might be much smaller.

The characteristic values of C_{irr} (Fig. 5), obtained for 4U 1543–47 (2002), are smaller comparing to ones usually derived on the theoretical and observational grounds. The irradiation factor C_{irr} should be $< 6 \times 10^{-4}$ in order for the hot-zone radius to be variable. On the other hand, [Dubus et al. \(2001\)](#) adopted $C_{\text{irr}} \sim 5 \times 10^{-3}$ to reproduce the light curves of X-ray novae. When analysing *Swift* optical/UV/X-ray broad-band data of XTE J1817–330 (the outburst of 2006), [Gierliński et al. \(2009\)](#) have found out that the spectra are consistent with a model of reprocessing a constant fraction of 10^{-3} of the bolometric X-ray luminosity (disk plus non-thermal tail), arguing in favour of the direct illumination of the black hole disk. For the 1999–2000 outburst of the BH transient XTE J1859+226, [Hynes et al. \(2002\)](#) have estimated the irradiation parameter $C_{\text{irr}} \sim 7.4 \times 10^{-3}$, assuming the accretion efficiency to be $\eta_{\text{accr}} = 0.1$.

Estimate (17) agrees with the value of C_{irr} for 4U 1543–47, assuming a presence of some relativistic focusing and the fact that the relative half-thickness z_0/r near R_{hot} at the peak reaches ~ 0.07 . There is no need to contrive ways for increasing the value given by (17). Instead, one has to answer a question what is the reason for C_{irr} being lower during the particular burst of this X-ray transient.

Figure 2 demonstrates that the disk was close to the Eddington limit in the 2002 outburst. Above the Eddington limit, outflows from the disk are expected ([Shakura & Sunyaev 1973](#)). There was possibly a weak outflow in 4U 1543–47 (2002), which was able to effectively attenuate X-rays. In principle, this may constrain C_{irr} in X-ray transients with about-Eddington accretion rates.

It is also possible that the factor C_{irr} depends on the proximity of R_{hot} to the tidal truncation radius of the disk. In short-period X-ray novae, R_{hot} at the peak is close to R_{tid} , while its peak value in 4U 1543–47 R_{hot} is apparently only about $(0.5 - 0.7) R_{\text{tid}}$.

6.2 Models with irradiation-controlled size of the hot zone

Figure 12 presents two attempts of modelling the decay of the 4U 1543–47 burst in 2002 in the assumption that the radius of the evolving disk remained constant. The plot illustrates that the assumption of constant size for the hot zone cannot in principle yield the observed shape of $\dot{M}(t)$, regardless of the values of R_{hot} and α .

The stage of irradiation-controlled hot zone with changing size was considered by [King & Ritter \(1998\)](#). The equation for the shrinking hot-zone mass,

$$\dot{M}_{\text{hot}} = -\dot{M}_{\text{in}} + \frac{d}{dt} (\Sigma(R_{\text{hot}}) \pi R_{\text{hot}}^2), \quad (18)$$

can be solved if one assumes a quasi-stationary evolution of the disk. In this case, $\dot{M}_{\text{hot}} \propto \Sigma(R_{\text{hot}}) R_{\text{hot}}^2$. The relationship (B1) between Σ and F and condition (8) for determining the radius R_{hot} of the hot zone yield the following power-law relationship between the mass of the hot part of the disk \dot{M}_{hot} and the inner accretion rate \dot{M}_{in} :

$$\dot{M}_{\text{in}} \propto \dot{M}_{\text{hot}}^{40/53} \quad (19)$$

(Kramers opacity). Expression (19) is fully confirmed by the FREDDI calculations. It can be deduced from (19) that $\dot{M} \propto (t_{\text{end}} - t)^{40/13}$, where t_{end} stands for the moment in time when the formal solution gives the zero disk mass. Notice that the consideration of this stage for the case, when the kinematic turbulent viscosity ν_t is independent of time and radius, yields $\dot{M} \propto (t_{\text{end}} - t)$ ('linear decay'; by [King & Ritter 1998](#)). However, variable ν_t is inherent for α -disks.

More involved numerical models used for calculating thermal stability and evolution of a disk with the irradiation-controlled cooling front (see, e.g., [Dubus et al. 2001](#)) suggest that the simple model

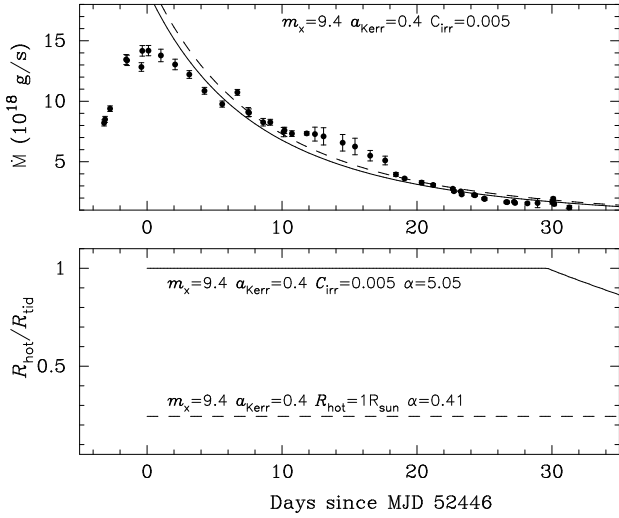


Figure 12. The evolution of a strongly-irradiated disk, $C_{\text{irr}} = 5 \times 10^{-3}$ (solid line), and evolution of a disk with the fixed radius of the hot zone (dashed line). Top panel: the accretion rate found by minimizing χ^2 , lower panel: the radius of the hot zone.

expressed by (18) may not provide fully reliable α values. The quasi-stationary approximation may prove to be too crude to accurately assess the velocity of the boundary of the uniform-viscosity zone.

To summarize, the model of the irradiation-controlled shrinking hot zone implemented in FREDDI describes the shape of $\dot{M}(t)$ in 4U 1543–47 quite satisfactorily. On the other hand, its current version probably overestimates α . Notice that the model of a completely ionized disk, also calculated by FREDDI, does not suffer from this shortcoming.

6.3 Determination of \dot{M} from observations

It is important to consider the general relativity effects when analysing the disk evolution in real systems. For given X-ray data, the peak accretion rate depends strongly on the Kerr parameter a_{Kerr} : \dot{M} changes by a factor of ~ 25 for $a_{\text{Kerr}} = 0 - 0.998$. This factor incorporates the variation of accretion efficiency of rotating black holes with different a_{Kerr} . Also, in the vicinity of a black hole, the outgoing X-ray spectrum is disturbed by the effects of Doppler boosting, gravitational focusing, and the gravitational redshift (Cunningham 1975).

In the present study, we use the spectral model of the relativistic disk *kerrbb* developed by Li et al. (2005). As mentioned by the authors, \dot{M} in *kerrbb* is the ‘effective’ accretion rate, while an actual one should be greater by a factor of $(1 + \eta_{\text{in.t.}})$, where $\eta_{\text{in.t.}}$ is the ratio of the disk heating due to a non-zero inner torque to the heating caused by the fall of accreting matter. For a non-rotating black hole, the magnetic torque at the inner edge of a thin magnetized accretion disk is only $\sim 2\%$ of the inward flux of the angular momentum (Shafee et al. 2008). In the present work, we assume $\eta_{\text{in.t.}} = 0$.

If the innermost stable circular orbit is $0.5 G M_x/c^2$ closer to the centre than a canonical value of $6 G M_x/c^2$ for a non-rotating black hole, as argued by Reynolds & Fabian (2008), then the related disk-power increase corresponds to a formal variation of a_{Kerr} from 0 to 0.15. As can be seen from Fig. 2, a higher Kerr parameter for the black hole translates into a smaller accretion rate. This un-

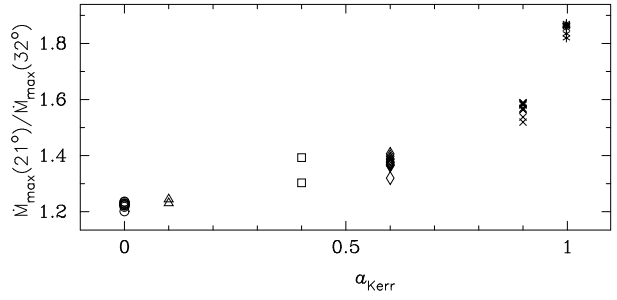


Figure 13. The ratio of the peak accretion rates of the 4U 1543–47 (2002) outburst for $i = 21^\circ$ and $i = 32^\circ$. The designations are the same as in Fig. 2. The dependence on a_{Kerr} is due to the relativistic focusing of X-rays.

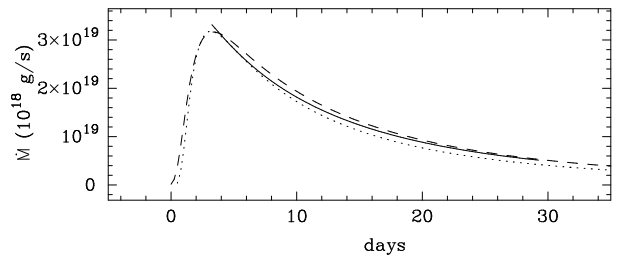


Figure 14. The modelled evolution of $\dot{M}(t)$ with different opacity implementations for the solar abundances: the dashed line is for Kramers law $\kappa = 5 \times 10^{24} \rho/T^{7/2} \text{ cm}^2 \text{ g}^{-1}$; the dotted line is for the analytic approximation to the OPAL tables $\kappa = 1.5 \times 10^{20} \rho/T^{5/2} \text{ cm}^2 \text{ g}^{-1}$ (Bell & Lin 1994); the solid line is calculated using the code of Malanchev & Shakura (2015) for the OPAL tables (Iglesias & Rogers 1996). Disk radius is constant, $C_{\text{irr}} = 0$.

certainty of relativistic disk models tends to be smaller for higher a_{Kerr} (Miller et al. 2009). In view of such uncertainties, we varied the Kerr parameters within some range to see how the results depended on them.

There are other modern XSPEC models for emission of the relativistic disk, for example, *kerrbb2* and *slimbb*, which are more sophisticated in some respects. However, these have the limitations that hinder us from using them: the *kerrbb2* model covers limited ranges for the accretion rate and spectral energy; *slimbb* has the luminosity as an input parameter, instead of the accretion rate.

6.4 Variation of the model assumptions

Results of spectral fitting by Morningstar & Miller (2014) suggest that the inclination of the inner disk in 4U 1543–47 differs from the binary inclination. When taking as the inclination the central value from the range derived by Morningstar & Miller (2014), $i = 32^\circ$, we obtain lower resulting accretion rates. The decrease depends on a_{Kerr} : it is $\sim 86\%$ for $a_{\text{Kerr}} = 0.998$ and $\sim 24\%$ for $a_{\text{Kerr}} = 0$ (Fig. 13). This inclination makes the resulting α smaller by a factor of 1.3 for $a = 0.998$ and by 1.1 for $a_{\text{Kerr}} = 0.0$ (for the Kramers opacity), as can be found from relationship (5).

Spectral modelling with the colour factor $f_{\text{col}} = 1$ gives systematically higher peak accretion rates and, thus, higher estimates for α .

In Fig. 14, we compare models with three different opacity implementations. The parameters of the disk are set as follows: $m_x = 10$, $\alpha = 0.5$, $R_{\text{hot}} = 10^{11} \text{ cm} = \text{const}$. We see that the difference in the opacity does not affect the results significantly in contrast to other uncertainties involved in the modelling.

7 SUMMARY

Bursts of X-ray novae are crucial laboratories to probe models of the non-stationary disk accretion. It is important therefore that a model of the viscous disk evolution takes into account the self-irradiation of the disk in a self-consistent way.

We assume the concept of the high turbulent parameter α in the hot ionized part of the disk and low α in the cold neutral zone. Coleman et al. (2016) have considered a dwarf-nova disk with $\alpha \sim 0.01$ in the ionized and neutral zones and with α one order higher in the zone with the partial ionization, following some recent results of numerical MHD simulations that have achieved a value of $\alpha \sim 0.1$ for the regions with the partial ionization and convection (Hirose et al. 2014). However, such low- α disks may face a difficulty at explaining the characteristic times of the exponential decays (several tens of days) and the time delays between the optical and X-ray band during outburst rises (several days), observed in some X-ray novae.

If an X-ray outburst is produced due to the variations of the central accretion rate in a completely ionized disk, a nearly exponential decay is expected for the disk with a constant outer radius. For such decays, which may take place in short-periodic X-ray novae, the turbulent parameter α can be estimated using analytic relationships (5)–(6) and the disk evolution can be calculated using the `FREDDI` code. Slower decays happen in the accreting viscous flows, which are radially expanding (ordinarily, this is not a case of a close binary system), or if a companion star provides additional matter to the disk. Faster decays are due to the progressive shrinking of the viscously-evolving zone (the zone with high α). Detailed modelling is needed to discriminate between these cases because the apparent similarity to an exponential decay may mask different scenarios.

The difference between the disk instability models proposed for explaining the bursts in dwarf and X-ray novae is thought to be mainly due to the major role of X-ray irradiation in the latter group of objects (e.g., van Paradijs & Verbunt 1984). The typical irradiation parameter $C_{\text{irr}} \sim 5 \times 10^{-3}$ was suggested (Dubus et al. 1999; Lasota et al. 2008).

We derived and analysed the accretion rate evolution $\dot{M}(t)$ during the first 30 days after the peak of 2002 outburst of 4U 1543–47, when it was in the high/soft state. We found that the observed evolution requires $\alpha \approx 3.2 - 3.3$ for the irradiation parameter $C_{\text{irr}} \sim 5 \times 10^{-3}$. This happens because the strong illumination leads to a large size of the hot part of the disk, and the short decay time can be obtained only with a high viscosity parameter. The shape of the $\dot{M}(t)$ curve of 4U 1543–47 (2002) cannot be produced by a hot zone with constant size; rather, it is consistent with the model of shrinking high-viscosity zone.

Putting aside mixed scenarios, there were two options depending on whether or not the central irradiating flux controlled the hot zone size. These corresponded to $C_{\text{irr}} \approx (3 - 6) \times 10^{-4}$ (‘mild irradiation’ case) and $C_{\text{irr}} \lesssim 1.5 \times 10^{-4}$ (‘no irradiation’ case) for 4U 1543–47 (2002). In the quasi-stationary model of the irradiation-controlled hot zone, we obtained $\alpha \sim 0.5 - 1.5$ for the range of the BH masses 6–10 M_{\odot} . The second case would resemble a decay in a dwarf nova disk and required $\alpha_{\text{hot}} \sim 0.08 - 0.32$.

The V and J light curves favour the value C_{irr} in the range $\sim (3 - 6) \times 10^{-4}$, making the model of irradiation-controlled hot zone in 4U 1543–47 more plausible. Nevertheless, there remains the possibility that the X-ray illumination can be of low importance for this and some other X-ray nova outbursts.

Table A1. Summary of spectral parameters used for two models: $TBabs * ((simpl * kerrbb + laor) * smedge)$ or $TBabs * (compTT + kerrbb + laor) * smedge$. The results obtained with values in brackets are discussed only in § 6.

Model component	Parameter	Value	
<i>TBabs</i> <i>kerrbb</i>	n_{H}	$4 \times 10^{21} \text{ cm}^{-2}$	
	$\eta_{\text{in.t.}} = F_{\text{in}} \omega_{\text{in}} / \eta_{\text{accr}} \dot{M} c^2$	0	
	a_{Kerr}	0, 0.6, 0.9, 0.998	
	i	20:7 (32°)	
	m_{x}	6, 7, 8, 9, 10	
	\dot{M}	$0 - 10^{21} \text{ g s}^{-1}$	
	d	$0 - 10^4 \text{ kpc}$	
	f_{col}	1.7 (1.0)	
	irradiation flag	1	
	limb-darkening flag	1	
	normalization	1	
	<i>simpl</i>	Γ	0 – 4.5
		f_{sc}	$10^{-3} - 0.3$
	<i>compTT</i>	only up-scattering flag	1
redshift		0	
T_0		$10^{-4} - 4 \text{ keV}$	
kT		$10 - 10^3 \text{ keV}$	
τ_{plasma}		$10^{-2} - 200$	
Geometry switch		disk	
<i>laor</i>	normalization	$0 - 10^{24} \text{ photons cm}^{-2} \text{ s}^{-1}$	
	E_{line}	5 – 7 keV	
	Index	3	
	R_{in}	$1.235 - 400 GM_{\text{x}}/c^2$	
	R_{out}	$400 GM_{\text{x}}/c^2$	
<i>smedge</i>	i	20:7 (32°)	
	normalization	$0 - 10^{24} \text{ photons cm}^{-2} \text{ s}^{-1}$	
	E_{edge}	6 – 10 keV	
	τ_{max}	0 – 10	
	Index	–2.67	
	Width	7 keV	

ACKNOWLEDGEMENTS

The authors are grateful to the anonymous referee for suggestions that have improved the clarity of the manuscript. The work is supported by the Russian Science Foundation grant 14-12-00146. Authors used the equipment funded by M.V. Lomonosov Moscow State University Program of Development.

APPENDIX A: SPECTRAL MODELLING

We analyse the archival data for the 2002 outburst of 4U 1543–47 obtained with the Proportional Counter Array aboard the *RXTE* observatory. We have selected the same data as in Park et al. (2004). In particular, long observations of 17, 19, 20, and 28 June 2002 were divided in two equal intervals. The ‘‘Standard-2’’ data from all Xe layers of PCU-2 have been used.

The basic reduction is made with the help of the `rex` script of HEASOFT 6.18. The background PCA model for bright sources is used. The good time intervals are selected according to the conservative options: the source elevation should have been greater than 10 degrees; the pointing offset, less than 0.02 degrees; 30 min should have elapsed after the observatory passage through the South Atlantic Anomaly. We calculate dead time corrections for the source and background to adjust the exposures, make re-

sponse matrices, and extract spectra using tools `pcadeadcalc2` and `pcaextspect2`.

The spectral fitting is done using XSPEC 12.9.0. Systematic errors of 1% are added via the command `system`. We use the absorption model `tbabs` with the hydrogen column $4 \times 10^{21} \text{ cm}^{-2}$ (according to the LAB (Kalberla et al. 2005) and GASS (Kalberla & Haud 2015) surveys; see AIfA Hi Surveys tool at Argelander-Institut für Astronomie) together with `wilm` abundances. The spectral fitting is carried out in the 2.9–25 keV interval.

To describe the thermal emission from the disk, the `kerrbb` spectral model is used. The spectral parameters can be found in Table A1. The accretion rate \dot{M} and the distance d are set free. We fix the BH mass M_x and the dimensionless Kerr parameter a_{Kerr} . The disk inclination is fixed and equal to 20:7 (Orosz 2003) or, alternatively, to 32° (Morningstar & Miller 2014), and the flux normalization is set to be unity. Flags for the disk irradiation and limb darkening are set on, and the two values of the colour factor f_{col} are tried: 1.7 and 1. Another fixed parameter is the zero-torque condition at the inner edge ($\eta_{\text{in.t.}} = 0$).

To describe the non-thermal component as the emission componentized in the high-temperature plasma near the disk, we use the convolution model `simpl` (Steiner et al. 2009). This empirical model, in which a fraction of seed photons produces the power-law component, can be used for any spectrum of the seed photons. The model has two free parameters: the photon power law index and the fraction of scattered photons. Since `simpl` redistributes input photons to higher and lower energies, the energy interval should be extended to adequately cover the relevant band. Following Steiner et al. (2009), we compute the model over 1000 logarithmically spaced energy bins between 0.05 and 50 keV. We hold the power-law index Γ between 0 and 4 and choose the ‘up-scattering’ mode.

As an alternative, we also model the power-law tail with `comptt` (Titarchuk 1994), which calculates the Compton scattering as a convolution using the scattering Green’s function. In `comptt`, we set free the seed photons’ and plasma temperatures, the optical depth, and the normalization parameter, choosing the ‘disk’ geometry.

Following Park et al. (2004), we include a spectral component to fit a broad edge-like absorption spectral feature. It is suggested that the feature near 7 keV is produced by the K-shell absorption of iron, smeared due to reflection or partial absorption of X-rays by the optically thick accretion disk (Ebisawa et al. 1994). The `smedge` spectral model reproduces the broadened Fe-absorption line (K-absorption structure) and should be multiplied with the continuum spectrum. We confine the parameter E_{edge} , which approximately corresponds to the energy of the iron K-edge (Ebisawa 1991), to values within 6 to 10 keV, and the smearing width parameter is fixed to be 7 keV, as in Park et al. (2004).

The spectral model `tbabs * (simpl * kerrbb) * smedge` gives acceptable fits (the reduced $\chi^2 < 1.5$) for the most spectra with chosen masses and Kerr parameters.

Park et al. (2004) have found an evidence of the Fe $K\alpha$ -line in the spectra of the source during the outburst. They have concluded that the XSPEC `laor` model that takes into account the relativistic effects leading to line broadening (Laor 1991) suits the line component better than the Gaussian model. We confirm this conclusion. In `laor`, the energy of the line centre is varied freely between 6.4 and 7 keV, following Park et al. (2004), while the inner radius is thawed. The other parameters, frozen by default, remain unchanged.

Morningstar & Miller (2014) have used the spectral component `relconv*reflionx` to describe the feature near 7 keV. We could not use it because the spectral component is not able to provide

satisfactory results at times close to the peak, apparently due to a limitation on the photon index in `reflionx`.

APPENDIX B: THE FREDDI CODE OVERVIEW

The FREDDI³ code is designed to solve the differential equation (1) with two boundary conditions on the viscous torque F : $F_{\text{in}} = 0$ and $(\partial F/\partial h)|_{\text{out}} = \dot{M}_{\text{out}} = 0$.

The code uses the analytic relationship between the surface density Σ and the viscous torque F :

$$\Sigma = \frac{(G M_x)^2 F^{1-m}}{4 \pi (1-m) D h^{3-n}}, \quad (\text{B1})$$

where m and n are the dimensionless constants that equal 3/10 and 4/5, respectively, for the Kramers opacity law, and 1/3 and 1, for $\kappa \propto \rho/T^{5/2}$ (Bell & Lin 1994), D is a diffusion coefficient (Lyubarskij & Shakura 1987; Suleimanov et al. 2008). The dimensional diffusion coefficient D in (B1) is approximately constant for specific disk parameters, as it depends on the parameter τ_0 (comparable to the disk optical thickness), and the dependence is rather weak for $\tau_0 \gg 1$ (Suleimanov et al. 2007). We use a constant value of D corresponding to $\tau_0 = 10^3$.

In FREDDI, the outer radius R_{hot} of the evolving disk can be varied so that either the effective temperature T_{eff} or the irradiation temperature T_{irr} would be constant. Thus, the shift of R_{hot} tracks the temperature variation. The outer boundary condition $\dot{M}_{\text{out}} = 0$ means that the distribution of the viscous torque in the outer cold disk is ignored.

To solve diffusion equation (1), it is necessary to know an initial distribution of either the function $F(h)$ or the function $\Sigma(h)$, where $h = \sqrt{G M_x r}$ is the specific angular momentum. FREDDI provides a possibility to choose one of the following initial distributions:

- Power law for the surface density: $\Sigma \sim \left(\frac{h-h_{\text{in}}}{h_{\text{out}}-h_{\text{in}}}\right)^{k_{\Sigma}}$.
- Power law for the viscous torque: $F \sim \left(\frac{h-h_{\text{in}}}{h_{\text{out}}-h_{\text{in}}}\right)^{k_F}$.
- Sinus law for the viscous torque: $F \sim \sin\left(\frac{h-h_{\text{in}}}{h_{\text{out}}-h_{\text{in}}}\frac{\pi}{2}\right)$. This law satisfies both border conditions for $F(h)$.
- Two-parametric Gaussian distribution for the viscous torque.
- Quasi-stationary distribution: $F \sim f_F\left(\frac{h}{h_{\text{out}}}\right)^{\frac{1-h_{\text{in}}/h}{1-h_{\text{in}}/h_{\text{out}}}}$, where $f_F\left(\frac{h}{h_{\text{out}}}\right)$ is a coordinate part of the self-similar analytic solution of the diffusion equation in the assumption of the fixed outer radius and zero inner radius (Lipunova & Shakura 2000).

All results presented in § 3.2 are obtained using the quasi-stationary distribution as the initial one.

Fig. 14 shows a comparison of the diffusion equation solutions obtained with FREDDI for different analytic opacity laws and the solution for tabulated opacity values (OPAL tables; Iglesias & Rogers 1996). We alternatively use the Kramers opacity $\kappa = 5 \times 10^{24} \rho/T^{7/2} \text{ cm}^2 \text{ g}^{-1}$ or $\kappa = 1.5 \times 10^{20} \rho/T^{5/2} \text{ cm}^2 \text{ g}^{-1}$ Bell & Lin (1994). The initial power-law distribution of the viscous torque with an index of $k_F = 6$ is set. The third solution (the solid line) is obtained with a code described in Malanchev & Shakura (2015) using tabulated OPAL opacities and a quasi-stationary initial distribution. The values of the disk parameters used in all of the three calculations are the same: $\alpha = 0.5$, $m_x = 10$, $a_{\text{Kerr}} = 0$, and

³ FREDDI – Fast Rise Exponential Decay: accretion Disk model Implementation. The code can be downloaded from <http://xray.sai.msu.ru/~malanchev/freddi/>

$R_{\text{hot}} = 10^{11}$ cm, the latter being taken constant. Figure 14 demonstrates that for this specific problem, both the solutions with the Kramers opacity law and the approximation by Bell & Lin (1994) provide a comparable accuracy in comparison with the solution with the table OPAL opacities.

The high speed of FREDDI and a specifically developed interface make it very useful for fitting the Shakura-Sunyaev α -parameter and the disk radius R_{hot} . One can set the distance d , the irradiation factor C_{irr} , and the inclination i of the system to obtain the X-ray flux and the spectral flux density at any wavelength. It should be noted that FREDDI uses an analytical vertical structure and thus works orders of magnitude faster than any other code, which uses tabulated opacity values and numerically solving the vertical structure equations. FREDDI has several tuning parameters: a time step, a number of coordinate steps and a type of coordinate grid (linear or logarithmic in terms of h). FREDDI is written on C++ and has a user-friendly command-line interface.

REFERENCES

- Arnaud K. A., 1996, in G. H. Jacoby & J. Barnes ed., *Astronomical Society of the Pacific Conference Series* Vol. 101, *Astronomical Data Analysis Software and Systems* V. pp 17–20
- Bell K. R., Lin D. N. C., 1994, *ApJ*, **427**, 987
- Buxton M. M., Bailyn C. D., 2004, *ApJ*, **615**, 880
- Cannizzo J. K., 1994, *ApJ*, **435**, 389
- Chandrasekhar S., 1961, *Hydrodynamic and hydromagnetic stability*. International Series of Monographs on Physics, Oxford: Clarendon, 1961
- Coleman M. S. B., Kotko I., Blaes O., Lasota J.-P., Hirose S., 2016, *MNRAS*, **462**, 3710
- Cox A., 2015, *Allen’s Astrophysical Quantities*. Springer New York, <https://books.google.ru/books?id=TjDtCAAQBAJ>
- Cunningham C. T., 1975, *ApJ*, **202**, 788
- Cunningham C., 1976, *ApJ*, **208**, 534
- Dubus G., Lasota J.-P., Hameury J.-M., Charles P., 1999, *MNRAS*, **303**, 139
- Dubus G., Hameury J.-M., Lasota J.-P., 2001, *A&A*, **373**, 251
- Ebisawa K., 1991, PhD thesis, Institute of Space and Astronautical Science/Japan Aerospace Exploration Agency
- Ebisawa K., et al., 1994, *PASJ*, **46**, 375
- Eggleton P. P., 1983, *ApJ*, **268**, 368
- Ertan Ü., Alpar M. A., 2002, *A&A*, **393**, 205
- Esin A. A., Kuulkers E., McClintock J. E., Narayan R., 2000, *ApJ*, **532**, 1069
- Gierliński M., Done C., Page K., 2009, *MNRAS*, **392**, 1106
- Hōshi R., 1979, *Progress of Theoretical Physics*, **61**, 1307
- Hawley J. F., Balbus S. A., 1991, *ApJ*, **376**, 223
- Hirose S., Blaes O., Krolik J. H., Coleman M. S. B., Sano T., 2014, *ApJ*, **787**, 1
- Hynes R. I., Haswell C. A., Chaty S., Shrader C. R., Cui W., 2002, *MNRAS*, **331**, 169
- Iglesias C. A., Rogers F. J., 1996, *ApJ*, **464**, 943
- Kalberla P. M. W., Haud U., 2015, *A&A*, **578**, A78
- Kalberla P. M. W., Burton W. B., Hartmann D., Arnal E. M., Bajaja E., Morras R., Pöppel W. G. L., 2005, *A&A*, **440**, 775
- Ketsaris N. A., Shakura N. I., 1998, *Astronomical and Astrophysical Transactions*, **15**, 193
- King A. R., Ritter H., 1998, *MNRAS*, **293**, L42
- King A. R., Pringle J. E., Livio M., 2007, *MNRAS*, **376**, 1740
- Kotko I., Lasota J.-P., 2012, *A&A*, **545**, A115
- Laor A., 1991, *ApJ*, **376**, 90
- Lasota J.-P., 2001, *New Astronomy Review*, **45**, 449
- Lasota J.-P., Dubus G., Kruk K., 2008, *A&A*, **486**, 523
- Li L.-X., Zimmerman E. R., Narayan R., McClintock J. E., 2005, *ApJS*, **157**, 335
- Lin D. N. C., Faulkner J., Papaloizou J., 1985, *MNRAS*, **212**, 105
- Lipunova G. V., 2015, *ApJ*, **804**, 87
- Lipunova G. V., Shakura N. I., 2000, *A&A*, **356**, 363
- Lyubarskij Y. E., Shakura N. I., 1987, *Soviet Astronomy Letters*, **13**, 386
- Lyutiy V. M., Sunyaev R. A., 1976, *Soviet Ast.*, **20**, 290
- Malanchev K. L., Shakura N. I., 2015, *Astronomy Letters*, **41**, 797
- Malanchev K. L., Postnov K. A., Shakura N. I., 2017, *MNRAS*, **464**, 410
- Menou K., Hameury J.-M., Stehle R., 1999, *MNRAS*, **305**, 79
- Mescheryakov A. V., Revnivtsev M. G., Filippova E. V., 2011, *Astronomy Letters*, **37**, 826
- Meyer F., 1984, *A&A*, **131**, 303
- Meyer F., Meyer-Hofmeister E., 1981, *A&A*, **104**, L10
- Meyer F., Meyer-Hofmeister E., 1984, *A&A*, **140**, L35
- Meyer F., Meyer-Hofmeister E., 1990, *A&A*, **239**, 214
- Miller J. M., Reynolds C. S., Fabian A. C., Miniutti G., Gallo L. C., 2009, *ApJ*, **697**, 900
- Morningstar W. R., Miller J. M., 2014, *ApJ*, **793**, L33
- Orosz J. A., 2003, in van der Hucht K., Herrero A., Esteban C., eds, *IAU Symposium* Vol. 212, *A Massive Star Odyssey: From Main Sequence to Supernova*. p. 365 ([arXiv:astro-ph/0209041](https://arxiv.org/abs/astro-ph/0209041))
- Orosz J. A., Jain R. K., Bailyn C. D., McClintock J. E., Remillard R. A., 1998a, *ApJ*, **499**, 375
- Orosz J. A., Jain R. K., Bailyn C. D., McClintock J. E., Remillard R. A., 1998b, *ApJ*, **499**, 375
- Orosz J. A., Polinsky E. J., Bailyn C. D., Tourtellotte S. W., McClintock J. E., Remillard R. A., 2002, *Bulletin of the American Astronomical Society*, **34**, 1124
- Paczynski B., 1977, *ApJ*, **216**, 822
- Park S. Q., et al., 2004, *ApJ*, **610**, 378
- Poutanen J., Veledina A., 2014, *Space Sci. Rev.*, **183**, 61
- Rahoui F., Lee J. C., Heinz S., Hines D. C., Pottschmidt K., Wilms J., Grinberg V., 2011, *ApJ*, **736**, 63
- Reynolds C. S., Fabian A. C., 2008, *ApJ*, **675**, 1048
- Ritter H., Kolb U., 2003, *A&A*, **404**, 301
- Russell D. M., Fender R. P., Hynes R. I., Brocksopp C., Homan J., Jonker P. G., Buxton M. M., 2006, *MNRAS*, **371**, 1334
- Shafee R., McKinney J. C., Narayan R., Tchekhovskoy A., Gammie C. F., McClintock J. E., 2008, *ApJ*, **687**, L25
- Shahbaz T., Charles P. A., King A. R., 1998, *MNRAS*, **301**, 382
- Shakura N. I., Sunyaev R. A., 1973, *A&A*, **24**, 337
- Smak J., 1984a, *Acta Astronomica*, **34**, 161
- Smak J., 1984b, *PASP*, **96**, 5
- Smak J., 2000, *New A Rev.*, **44**, 171
- Steiner J. F., Narayan R., McClintock J. E., Ebisawa K., 2009, *PASP*, **121**, 1279
- Suleimanov V., Meyer F., Meyer-Hofmeister E., 1999, *A&A*, **350**, 63
- Suleimanov V., Meyer F., Meyer-Hofmeister E., 2003, *A&A*, **401**, 1009
- Suleimanov V. F., Lipunova G. V., Shakura N. I., 2007, *Astronomy Reports*, **51**, 549
- Suleimanov V. F., Lipunova G. V., Shakura N. I., 2008, *A&A*, **491**, 267
- Titarchuk L., 1994, *ApJ*, **434**, 570
- Tuchman Y., Mineshige S., Wheeler J. C., 1990, *ApJ*, **359**, 164
- Velikhov E. P., 1959, *Soviet Journal of Experimental and Theoretical Physics*, **9**, 995
- Vishniac E. T., Wheeler J. C., 1996, *ApJ*, **471**, 921
- van Paradijs J., Verbunt F., 1984, in Woosley S. E., ed., *American Institute of Physics Conference Series* Vol. 115, *American Institute of Physics Conference Series*. pp 49–62, [doi:10.1063/1.34556](https://doi.org/10.1063/1.34556)